



UNIVERSIDADE ESTADUAL DE CAMPINAS  
SISTEMA DE BIBLIOTECAS DA UNICAMP  
REPOSITÓRIO DA PRODUÇÃO CIENTÍFICA E INTELLECTUAL DA UNICAMP

**Versão do arquivo anexado / Version of attached file:**

Versão do Editor / Published Version

**Mais informações no site da editora / Further information on publisher's website:**

<https://www.sciencedirect.com/science/article/pii/S0140700718303931>

**DOI: 10.1016/j.ijrefrig.2018.10.008**

**Direitos autorais / Publisher's copyright statement:**

©2019 by Elsevier. All rights reserved.

DIRETORIA DE TRATAMENTO DA INFORMAÇÃO

Cidade Universitária Zeferino Vaz Barão Geraldo

CEP 13083-970 – Campinas SP

Fone: (19) 3521-6493

<http://www.repositorio.unicamp.br>



## Optimization of a vapor injection refrigeration cycle using hydrocarbon mixed refrigerants

Stella Maia Rocha de Carvalho, Luiz Henrique Parolin Massuchetto, Raiza Barcelos Corrêa do Nascimento, Hugo Valença de Araújo, José Vicente Hallak d'Angelo\*

Department of Chemical Systems Engineering, School of Chemical Engineering, University of Campinas, Av. Albert Einstein, 500, Bloco A, Campinas, São Paulo CEP 13083-852, Brazil

### ARTICLE INFO

#### Article history:

Received 18 July 2018

Revised 1 October 2018

Accepted 8 October 2018

Available online 1 November 2018

#### Keywords:

Refrigeration

Simulation

Vapor injection

Mixed refrigerant

Hydrocarbons

Optimization

### ABSTRACT

Refrigeration systems are major consumers of electrical energy in many process industries. Hydrocarbons have regained interest as refrigerants because of the increasing restrictions applied to halogenated fluids. In this work, the use of hydrocarbons mixed refrigerants and an alternative flash tank with vapor injection (FTVI) refrigeration cycle were combined. Five different binary mixed refrigerants involving R170 (ethane), R290 (propane), R600 (n-butane) and R600a (isobutane) were studied. Using different refrigerant compositions, the cycle was simulated and optimized for maximum COP, considering a fixed refrigeration capacity in the evaporator to reduce the temperature of a secondary thermal fluid from 281.55 K to 269.15 K. Parameters analyzed were: coefficient of performance, temperature glide in the evaporator and refrigerant mass flow rate. The use of a FTVI led to a COP improvement from 4% to 36% when compared to the traditional vapor compression cycle (VCC). The pair R290/R600 with 60/40 wt% presented the maximum COP of 4.88.

© 2018 Elsevier Ltd and IIR. All rights reserved.

## Optimisation d'un cycle frigorifique à injection de vapeur en utilisant un mélange de frigorigènes hydrocarbures

Mots-clés: Froid; Simulation; Injection de vapeur; Mélange de frigorigènes; Hydrocarbures; Optimisation

### 1. Introduction

Refrigeration systems are intensively present nowadays society in domestic, commercial and industrial applications. Estimates show that there are roughly 3 billion of refrigeration, air-conditioning and heat pump equipment in operation in the world and they are responsible for the consumption of almost 17% of electrical power worldwide (IIR, 2015). For this reason, constant efforts have been made towards increasing the efficiency of these systems, since even relatively small improvements in their per-

formance might have a significant impact in energy consumption also affecting the costs involved in their acquisition, maintenance and operation. Energy savings in refrigeration systems can be accounted through its coefficient of performance (COP), which is the ratio between the cooling capacity and the total energy demanded by the system.

The most common refrigeration cycle is the conventional vapor compression cycle (VCC) and one approach to search for refrigeration cycles with higher performance is the use of alternative cycles. These cycles might differ from the VCC in their operational principles – as the absorption cycle – or simply introducing variations like the ejector, cascade and refrigerant injection cycles. However, altering the cycle tends to increase not only its COP but also capital costs and operational complexity of the refrigeration system. Computational simulations allow comparison between possible alternatives in a faster and cheaper way, exploring dif-

\* Corresponding author.

E-mail addresses: [stellamrc@feq.unicamp.br](mailto:stellamrc@feq.unicamp.br) (S.M.R. de Carvalho), [luizhpmas@gmail.com](mailto:luizhpmas@gmail.com) (L.H.P. Massuchetto), [raiza.b.nascimento@gmail.com](mailto:raiza.b.nascimento@gmail.com) (R.B.C. do Nascimento), [hugoaraujo@feq.unicamp.br](mailto:hugoaraujo@feq.unicamp.br) (H.V. de Araújo), [dangelo@feq.unicamp.br](mailto:dangelo@feq.unicamp.br) (J.V.H. d'Angelo).

## Nomenclature

$a_i$	parameter “a” of the PR-EOS for the pure component “i” ( $\text{m}^6 \text{kPa mol}^{-2}$ )
$a_{\text{mix}}$	parameter “a” of the PR-EOS obtained by mixing rules ( $\text{m}^6 \text{kPa mol}^{-2}$ )
$b_{\text{mix}}$	parameter “b” of the PR-EOS obtained by mixing rules ( $\text{m}^3 \text{mol}^{-1}$ )
$\text{COP}_{\text{gain}}$	relative increment in the COP of a FTVI cycle compared to the one of a VCC (%)
$h_i$	specific enthalpy of stream “i” ( $\text{kJ kg}^{-1}$ )
$k_{ij}$	binary interaction parameter for PR-EOS mixing rule
$\dot{m}_i$	mass flow rate of stream “i” ( $\text{kg s}^{-1}$ )
$M_{\text{HYSYS}}$	the value of a property taken from Aspen Hysys® databank
$M_{\text{Reference}}$	the value of a property taken from the REFPROP®
$P_{\text{critical}}$	critical pressure (kPa)
$P_i$	pressure of stream “i” (kPa)
$Q_{\text{evaporator}}$	rate of heat exchange or cooling capacity in the evaporator (kW)
RTG	refrigerant temperature glide (K) or ( $^{\circ}\text{C}$ )
$T$	temperature (K) or ( $^{\circ}\text{C}$ )
$T_{\text{cond}}$	temperature at the condenser outlet stream ( $^{\circ}\text{C}$ )
$T_{\text{critical}}$	critical temperature (K)
$T_{\text{discharge}}$	compressor discharge temperature ( $^{\circ}\text{C}$ )
$T_{\text{evap}}$	temperature at the evaporator outlet stream ( $^{\circ}\text{C}$ )
$T_i$	temperature of process stream “i” (K) or ( $^{\circ}\text{C}$ )
$T_{\text{sat\_liq}}$	saturated liquid temperature (K)
$T_{\text{sat\_vap}}$	saturated vapor temperature (K)
$V_{\text{critical}}$	critical volume ( $\text{m}^3 \text{kmol}^{-1}$ )
$W_{\text{compressor}}$	compressor power input in the VCC (kW)
$\dot{W}_{\text{comp1}}$	compressor power input in the first stage of the FTVI (kW)
$\dot{W}_{\text{comp2}}$	compressor power input in the second stage of the FTVI (kW)
$x_i$	molar fraction of component “i”
$x_{\text{inj}}$	injection ratio – ratio between molar flows
$Z_{\text{critical}}$	critical compressibility factor
$\omega$	acentric factor
$\Delta h_{\text{vap}}$	specific evaporation enthalpy ( $\text{kJ kg}^{-1}$ )
$\Delta T_{\text{evaporator}}$	refrigerant temperature difference – evaporator inlet and outlet streams (K)
$\Delta T_{\text{HXF}}$	temperature variation of the heat exchange fluid in the evaporator (K)
$\Delta T_{\text{min}}$	minimum temperature approach adopted in heat exchangers (K)

## Acronyms

COP	coefficient of performance
CR	compression ratio in a compressor
ER	expansion rate in a valve
FTVI	flash tank vapor injection refrigeration cycle
GWP	global warming potential
HC	hydrocarbon
HXF	heat exchange fluid
HYSYS	process simulation software Aspen Hysys® version 8.4
ODP	ozone depletion potential
PR-EOS	Peng–Robinson equation of state
VCC	vapor compression cycle
VLE	vapor–liquid equilibrium

ferent options, helping to decide if further investigations of some studied refrigeration systems are worthwhile.

The alternative cycle studied in this work is the flash tank with vapor injection (FTVI) refrigeration cycle, which differs from the VCC by the addition of a second compression stage and a flash tank that allows vapor injection between compression stages. Many authors have reported that injection cycles present better performance than the VCC. For example, Heo et al. (2010) compared a conventional cycle with a vapor injection one for heat pump application. The utilization of the vapor injection enhanced heating capacity and COP by 10% and 25%, respectively. Xu et al. (2011) and Park et al. (2015) presented reviews on the benefits and advantages of an FTVI (among other injection cycles) in comparison to the VCC.

Recently, Qi et al. (2017) have studied a novel hybrid vapor injection cycle with subcooler and flash tank for air-source heat pumps, applying an ejector to combine both advantages of the subcooler and the flash tank vapor injection. Simulations indicated that the COP of this system, operating with R290 can be increased around 3% when compared to a conventional subcooler vapor injection cycle and around 1.5% when compared to an FTVI. Xu et al. (2017) performed an experimental investigation on heating performance of an FTVI using R32, R1234yf and their 20/80 wt% mixture, concluding that COP can be improved from 13% to 16% when compared to a system with no vapor injection. Xu et al. (2018) reported the use of a newly designed vapor-injected heat pump using injection subcooling, which was developed from the conventional FTVI, operating with R32 and heating COP was increased around 13% when compared to a system operating with liquid injection. Tello-Oquendo et al. (2018) presented a comprehensive study of two-stage vapor compression cycles with vapor-injection for several pure refrigerants considering that the heat sink has a limited capacity.

The choice of the refrigerant fluid is also important since it is related not only to the thermodynamic performance of the cycle but also to its environmental impact, which is commonly evaluated by metrics like ODP (Ozone Depletion Potential) and GWP (Global Warming Potential). However, as the operation of the refrigeration cycle itself also impacts on global warming by demanding electrical energy, the thermodynamic cycle efficiency given by its COP is closely related to the environmental impact. Alternative refrigerants, like hydrocarbons (HC), have regained attention for having low environmental impact and thermodynamic characteristics that contribute to consider them as potential and efficient fluids to replace halogenated refrigerants (Calm, 2008).

Palm (2008) evaluated the thermodynamic and physical properties of some HCs in comparison with halogenated refrigerants, concluding that HCs present better characteristics, such as higher vaporization enthalpy and thermal conductivity and lower viscosity. These characteristics contribute to improve the performance of the refrigeration systems and reduce the size of the equipment involved, especially heat exchangers. In addition, hydrocarbons have zero ODP, low GWP and are non-toxic. The main drawback of this refrigerant class is its high flammability, which limits the refrigerant charge in the system and increases safety requirements of building and operation.

The use of mixed refrigerants is one way to achieve some necessary operating condition. Refrigerant mixtures may be azeotropic or zeotropic (non azeotropic). The phase change behavior of the first is similar to that of a pure component, but zeotropic mixtures present temperature and phase composition variation during evaporation, which has a great influence on the thermodynamic performance of the cycle. Didion and Bivens (1990), Heberle et al. (2012) and Deethayat et al., (2015) showed that the use of zeotropic mixtures as refrigerants can contribute with the reduction of irreversibility during heat transfer in heat exchangers. This

is due to the temperature glide occurred during the phase change at a constant pressure, allowing manipulation of composition to better match the temperature profile between heat exchanging streams.

Mohanraj et al. (2009) performed an experimental study analyzing the substitution of R134a by a mixture of propane (R290) and isobutane (R600a) for a domestic refrigerator. They concluded that the blend of R290/R600a 45.2/54.8 wt% presented lower energy consumption than R134a and a COP improvement of 3.6%. Park and Jung (2007) studied the replacement of R22 for pure hydrocarbons and mixtures. The mixture composed of R1270/R290/R-E170 45/40/15 wt% presented the best performance, with a COP 5.7% higher than R22. More recently, Zheng and Wei (2018) have realized a performance analysis of a novel vapor injection enhanced by a cascade condenser for zeotropic mixtures to liquefy the separated vapor stream in the flash tank. They have performed simulations based on R290/R600a 50/50 wt% mixed refrigerant indicating that their cycle obtained a COP 2.6% higher than the one of a traditional FTVI.

Although comprehensive literature exists about the use of FTVI as alternative refrigeration cycle and HC mixtures as alternative refrigerants, there are not many works dealing with the combination of these both alternatives. The use of non azeotropic mixtures in a cycle with a flash separation tank leads to different refrigerant composition along the cycle and may present interesting consequences over the cycle's efficiency and operation depending on the application.

A parametric analysis of an FTVI cycle operating with propane/isobutane mixtures was presented by d'Angelo et al. (2016), where the evaporator and condenser temperatures were fixed at  $-23.3^{\circ}\text{C}$  and  $54.4^{\circ}\text{C}$ , respectively and the compositions with 30–50 wt% of propane has presented the best COP and the injection cycle presented gains in COP between 16% and 32% when compared to the conventional VCC.

Araújo et al. (2016) performed an exergetic analysis of the same system and reported that the evaporator accounted for almost 24% of the exergy losses for the best performing refrigerant mixture. These studies, however, did not considered an optimization of the cycle temperatures around the demands of a specific application. The matching of the temperature profiles between the refrigerant and the thermal fluid in the heat exchanger can reduce the exergy losses in heat exchangers, contributing to a better cycle performance.

In this work, VCC and FTVI were simulated operating with binary mixtures of hydrocarbons as refrigerant fluids. Mixed refrigerants studied are: R170/R290; R170/R600; R170/R600a; R290/R600 and R290/R600a.

The use of natural refrigerants to retrofit and modify existing cooling and heating systems requires extensive investigations before proceeding with these modifications. There are not so many works dealing with mixed refrigerants involving hydrocarbons (HCs), so this work may bring a contribution to understand and explore the performance of some mixed refrigerants using HCs. The choice of these natural refrigerants was based mainly on the fact that they form non-azeotropic mixtures (except R600 and R600a) and because of their availability, low cost and low environmental impact.

The application studied is the cooling rate needed between fermentation and maturation stages in the brewing process. This application was chosen as a reference to evaluate refrigeration system requirements. The main objective of this work is to find the best mixed refrigerant composition and operating conditions of the FTVI cycle, that lead to the maximum COP value. This work brings additional contributions to the previous work done by d'Angelo et al. (2016), including two different refrigerants (R170/ethane and R600/n-butane) and performing an optimization procedure for

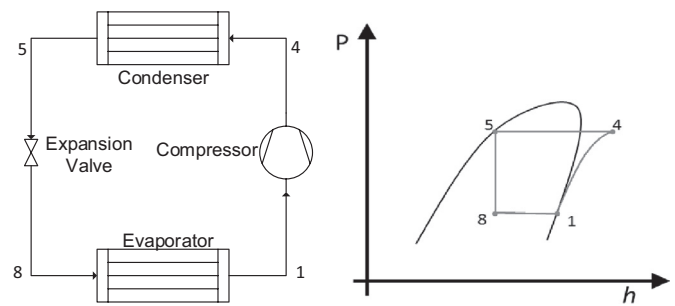


Fig. 1. Scheme of a vapor compression cycle (VCC) and its  $P$ - $h$  diagram.

maximum COP and not only a parametric analysis like in the former work.

## 2. Methodology

### 2.1. Cycle description

Fig. 1 presents the scheme of a conventional vapor compression cycle (VCC) with its four basic components (condenser, expansion valve, evaporator and compressor) and its respective pressure-enthalpy diagram. In this conventional cycle, refrigerant composition is the same in all process streams. The main difference from a VCC operating with pure and mixed refrigerants is that when a refrigerant mixture is used it will present a temperature variation along evaporation and condensation processes, while for pure refrigerants temperature is constant when a phase change occurs.

In the VCC cycle a saturated liquid stream (#5) at the condenser outlet expands producing a two-phase (liquid–vapor) stream (#8) that feeds the evaporator. In the evaporator, heat is removed from a secondary thermal fluid to the refrigerant, vaporizing it. Evaporator outlet stream (#1) is saturated vapor, which feeds the compressor, where temperature and pressure are increased, producing a superheated vapor stream (#4), that feeds the condenser, closing the cycle (the sequence of the numbers 1–4–5–8 is due to the ones used in the FTVI as will be explained).

The flash tank with vapor injection (FTVI) refrigeration cycle consists in a modification of the VCC where a flash separator is introduced in the cycle after the expansion valve, as shown in Fig. 2. The liquid–vapor mixture generated in the expansion process is separated in the flash tank, which has two output streams: a vapor stream (#9) and a liquid stream (#2). When a mixed refrigerant is used, stream #9 will be more concentrated in the lighter component and stream #2 will be more concentrated in the heavier one, so they will present a distinct composition, differently when a pure refrigerant is used. In Fig. 2 the pressure-enthalpy diagram of an FTVI for a pure refrigerant is presented together with the scheme of the cycle, identifying all process streams. As can be seen, this cycle uses two compression stages and two expansion valves. The top stream of the flash tank (#9) is saturated vapor and it is mixed with the vapor stream that comes from the first compression stage (#2) before feeding the second compression stage. This mixture between streams #9 and #2 contributes to reduce the temperature, causing a decrease in the total compression power required in both the compressors.

Fig. 3 shows the pressure-enthalpy diagram of a FTVI cycle operating with a zeotropic mixed refrigerant. Considering that for each composition of the zeotropic mixed refrigerant at stream #5 there is a specific phase composition for a fixed temperature and pressure at the outlet streams in the flash tank, the pressure-enthalpy diagram of the FTVI cycle needs to take into consideration that there are three different composition ranges in the cycle:

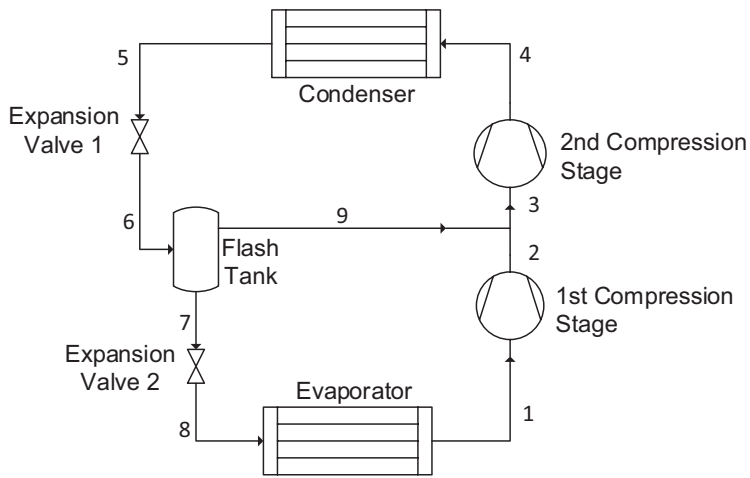


Fig. 2. Scheme of a FTVI refrigeration cycle and its P-h diagram for a pure refrigerant.

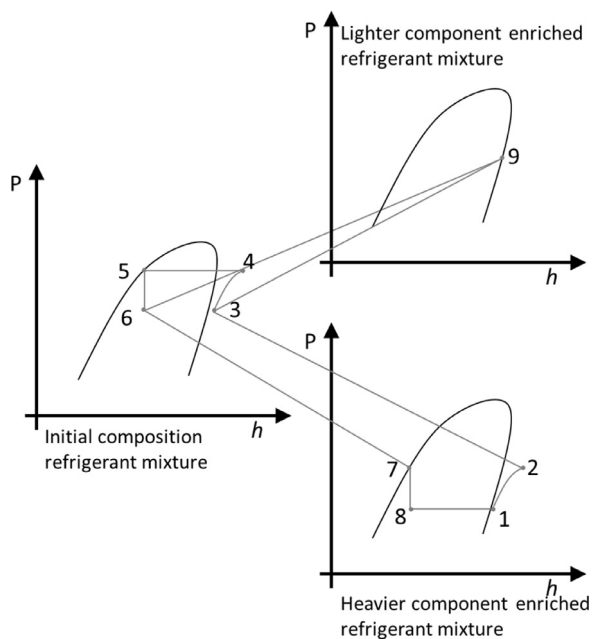


Fig. 3. P-h diagram of a FTVI cycle operating with zeotropic refrigerant mixture.

one from streams #3 to #6, another from streams #8 to #2 and stream #9.

The FTVI cycle can be described by the following steps:

- a saturated liquid stream (#5) of mixed refrigerant undergoes through an isenthalpic expansion producing stream #6, a liquid–vapor mixture at an intermediate pressure that feeds the flash tank;
- vapor and liquid phases in stream #6 are separated in the flash tank at constant pressure, producing a saturated vapor stream in the top (#9), which is enriched in the lighter component and a saturated liquid stream in the bottom (#7) enriched in the heavier component; both streams are at the same pressure and temperature;
- stream #7 is expanded through a second isenthalpic valve leading to a new partial vaporization, lowering pressure even more, producing a new liquid–vapor stream (#8), reaching the lowest temperature of the cycle as well;
- stream #8 is fed into the evaporator producing the desired refrigeration effect over a secondary thermal fluid that exchange heat with the mixed refrigerant. Temperature variation along

- this evaporation process depends on both initial refrigerant composition (the basis of calculation is taken at stream #5) and the expansion ratio in the first isenthalpic valve. Stream #8 is evaporated turning into a saturated vapor stream (#1);
- stream #1 is compressed in the first compression stage from the lowest pressure to an intermediate one reaching a state of superheated vapor at stream #2;
- streams #2 and #9, both at the intermediate pressure, are mixed in a chamber, generating stream #3, reestablishing the original mixed refrigerant composition of stream #5. Stream #3 is superheated vapor at the same pressure of streams #2 and #9 and it is fed into the second compression stage;
- the second compression stage raises temperature and pressure of stream #3 reaching the highest pressure level of the cycle, producing an outlet stream of superheated vapor (#4);
- stream #4 is fed into the condenser being cooled by a cold utility. Mixed refrigerant condenses at constant pressure while undergoing a temperature decrease, which depends on the refrigerant composition, producing stream #5, closing the cycle.

Due to the flash separation at intermediate pressure and an additional expansion stage of the liquid phase, the liquid–vapor mixture entering the evaporator has a lower enthalpy when compared to a single-stage refrigeration cycle as in the case of a VCC. The increase in the enthalpy variation along the evaporator decreases refrigerant mass flow rate for a fixed cooling capacity. In this case, for a fixed compression ratio (taken as the ratio between the highest and the lowest pressures in the cycle), the compression done in two stages, instead of using only one (as is the case of a VCC), requires a lower total compression power.

When a zeotropic mixture is used as refrigerant, phase transitions under constant pressure do not occur at constant temperature. The observed temperature glide in the heat exchangers of the VCC and FTVI depend on the temperature levels between which the cycle operates and on the initial refrigerant composition chosen. In the FTVI evaporator, the glide also depends on the expansion ratio in valve 1, since it is directly related to the composition of the liquid and vapor streams that are separated in the flash tank.

In addition, due to the refrigerant temperature glide, in order to compare the thermodynamic performance of cycles operating with zeotropic mixtures, it is necessary to define not only evaporation and condensation temperatures, but also where they will be specified (McLinden and Radermacher, 1987). In this work, the reference points chosen were evaporator inlet stream (#8) and saturated vapor temperature inside the condenser.

## 2.2. Modeling

The refrigerant cycles were studied by means of simulations, using software Aspen HYSYS® version 8.4 from AspenTech (2018) and the following assumptions were considered in the simulations of both VCC and FTVI cycles:

- steady state operation;
- negligible pressure drop in pipes, heat exchangers and in the flash tank;
- all equipment are adiabatic, with no heat losses to the surroundings;
- saturated liquid state at condenser outlet stream (#5);
- saturated vapor state at evaporator outlet stream (#1);
- streams #7 (liquid) and #9 (vapor) are in thermodynamic equilibrium at the same temperature and pressure;
- a cooling capacity of 1 kW (3600 kJ h<sup>-1</sup>) is fixed to allow easier scale changes;
- an isentropic efficiency of 80%, based on recommended values by Campbell (1992) and Oh et al. (2016), is adopted for all compression stages;
- expansion valves are isenthalpic;
- heat exchanger fluid (HXF) in the evaporator (also referred to as secondary refrigerant or thermal fluid) was considered a solution of water/ethanol 75/25 wt%. This fluid enters the evaporator at 281.55 K (8.4 °C) and leaves it at 269.15 K (−4 °C). These temperatures were defined based on the ones needed between fermentation and maturation stages in a brewing process;
- condenser is refrigerated by water, which is fed at 298.15 K (25 °C) leaving at 308.15 K (35 °C);
- a minimum temperature approach of 5 °C is adopted in both heat exchangers. This choice was based on the recommendation given by Heggs (1989) and Oh et al. (2016).

Input variables defined in this work are: expansion ratio in valve 1; evaporation and condensation temperatures and refrigerant composition (in wt%). Several scenarios with different refrigerant composition were simulated, while the ER and temperatures were optimized for each scenario. Expansion ratio (ER) in the upper stage valve is calculated by Eq. (1), where  $P$  is the pressure of the stream indicated in the subscript. ER was calculated in the range from 10 to 80% because higher ER values are not feasible, while lower ones make FTVI tend to VCC.

$$ER(\%) = \left( \frac{P_5 - P_6}{P_5} \right) \times 100 \quad (1)$$

Mixed refrigerants studied are composed exclusively by hydrocarbons within a homologous series (ethane, propane, isobutane and n-butane). Methane was excluded because its critical temperature is too low for the defined system and temperatures, which would require a different cooling strategy. Pentane, for its turn, leads to pressures under the atmospheric at the evaporator temperature, which would demand significant changes in the system. Except for the system (butane/isobutane) which forms an azeotropic mixture, all other binary combinations between the chosen refrigerant were tested. For each pair, composition was varied with intervals of 10%, ranging from one pure fluid to another.

As mentioned before, simulations of both VCC and FTVI were developed using process simulator Aspen Hysys® and the thermodynamic package chosen was the Peng–Robinson equation of state (PR-EOS), which is specially indicated for hydrocarbons (Peng and Robinson, 1976). This simulator was chosen because of its reliability and potential to evaluate the performance of complex industrial processes, also allowing optimization procedures using some software built-in tools.

The binary interaction parameter ( $k_{ij}$ ) was estimated internally from the process simulator databank and the mixing rules used are the standard ones for PR-EOS, i.e.,  $a_{mix} =$

**Table 1**

Binary interaction parameters of studied refrigerant pairs (Aspen Hysys®).

$k_{ij} \cdot 10^3$	Ethane	Propane	Isobutane	n-Butane
Ethane	–	1.260	4.570	4.100
Propane	1.260	–	1.040	0.819
Isobutane	4.570	1.040	–	0.470
n-Butane	4.100	0.819	0.470	–

$\sum_{i=1}^n \sum_{j=1}^n x_i x_j (a_i a_j)^{0.5} (1 - k_{ij})$  and  $b_{mix} = \sum_{i=1}^n x_i b_i$ , where  $i$  and  $j$  are the pure components of the mixture constituted of  $n$  components,  $x_i$  and  $x_j$  are the mole fraction of components  $i$ ,  $j$  and  $a_i$ ,  $b_i$  are the PR-EOS parameters for pure components. Table 1 presents the values of the binary interaction parameters for the systems studied in this work.

The coefficient of performance was calculated from Eq. (2) for the VCC and (3) for the FTVI cycle, while Eq. (4) allows the calculation of mass flow rate of refrigerant, considering the specific enthalpies of streams #1 and #8 and the fixed cooling rate at the evaporator, which was fixed as 1 kW. Refrigerant temperature glide (RTG) is defined by Eq. (5).

$$COP = \frac{\dot{Q}_{evaporator}}{\dot{W}_{compressor}} \quad (2)$$

$$COP = \frac{\dot{Q}_{evaporator}}{\dot{W}_{comp1} + \dot{W}_{comp2}} \quad (3)$$

$$\dot{Q}_{evaporator} = \dot{m}_1 (h_1 - h_8) \quad (4)$$

$$RTG = T_{sat\_vap} - T_{sat\_liq} \quad (5)$$

## 2.3. Model validation

The model used in this work was validated using three different criteria: checking pure components properties of the simulator databank; comparison of calculated vapor–liquid equilibrium data with literature experimental data and comparison of thermodynamic cycle performance obtained in simulations with the ones reported in the literature.

The properties of the pure components checked were critical data (temperature, pressure, volume and compressibility factor), acentric factor and saturation pressure at some temperatures. These data were extracted from Aspen HYSYS® databank and compared to data taken from REFPROP® version 9.11, which is considered a reliable reference for refrigerant data and widely used in works dealing with refrigeration systems simulations. Table 2 presents the values of these properties for both databanks and the deviation between them, which is calculated by Eq. (6), where  $M$  represents a generic property. All compared values were fairly close, with maximum deviation around 2.5% which was considered very satisfactory.

$$Deviation(\%) = \frac{|M_{reference} - M_{Hysys}|}{M_{reference}} \times 100 \quad (6)$$

Data for saturation pressure of pure components at the temperatures of −50, −25, 0, 25, 50, 75 °C (when pertinent) was also evaluated and again compared to the ones taken from REFPROP®. Maximum deviation found was less than 2% as can be seen in Table 3. Once again thermodynamic data calculated by Aspen Hysys® can be considered very satisfactory, indicating that the behavior of pure fluids will be correctly simulated.

The second step of the validation process was a comparison of vapor–liquid equilibrium (VLE) data estimated by the PR-EOS, which was the thermodynamic package chosen for the simulations and VLE data taken from the literature. An appropriate VLE

**Table 2**  
Comparison of pure refrigerants critical data and acentric factor between Aspen Hysys® v.8.4 and REFPROP® v.9.11 databanks.

Component	Databank	$T_{critical}$ (K)	$P_{critical}$ (kPa)	$V_{critical}$ (m <sup>3</sup> kmol <sup>-1</sup> )	$\omega$	$Z_{critical}$
Ethane	HYSYS	305.43	4884.0	0.1480	0.0986	0.285
	REFPROP	305.32	4872.2	0.1458	0.0995	0.280
	Deviation	0.04	0.24	1.48	0.90	1.69
Propane	HYSYS	369.90	4257.0	0.2000	0.1524	0.277
	REFPROP	369.89	4251.2	0.2000	0.1521	0.276
	Deviation	0.00	0.14	0.00	0.20	0.13
n-Butane	HYSYS	425.15	3797.0	0.2550	0.2010	0.274
	REFPROP	425.13	3796.0	0.2549	0.2010	0.274
	Deviation	0.00	0.03	0.03	0.00	0.05
Isobutane	HYSYS	408.05	3648.0	0.2630	0.1848	0.283
	REFPROP	407.81	3629.0	0.2577	0.1840	0.276
	Deviation	0.06	0.52	2.04	0.43	2.51

**Table 3**  
Saturation pressure (kPa) for pure refrigerants at different temperatures obtained by Aspen Hysys® v. 8.4 and REFPROP® v. 9.11.

Component	Databank	Temperature (°C)					
		-50	-25	0	25	50	75
Ethane	HYSYS	552.5	1237.3	2401.1	4209.5	-	-
	REFPROP	551.8	1233.5	2386.7	4190.3	-	-
	Deviation	0.13	0.31	0.60	0.46	-	-
Propane	HYSYS	71.0	203.3	473.5	952.3	1720.4	2868.4
	REFPROP	70.6	203.4	474.5	952.1	1713.3	2849.3
	Deviation	0.64	0.08	0.20	0.03	0.41	0.67
n-Butane	HYSYS	9.6	36.0	102.8	241.9	493.8	905.9
	REFPROP	9.5	35.9	103.2	243.3	495.8	906.2
	Deviation	1.73	0.25	0.40	0.55	0.39	0.03
Isobutane	HYSYS	17.1	58.5	156.0	348.0	681.3	1209.6
	REFPROP	16.8	58.4	157.0	350.7	684.9	1210.7
	Deviation	1.87	0.12	0.63	0.76	0.52	0.09

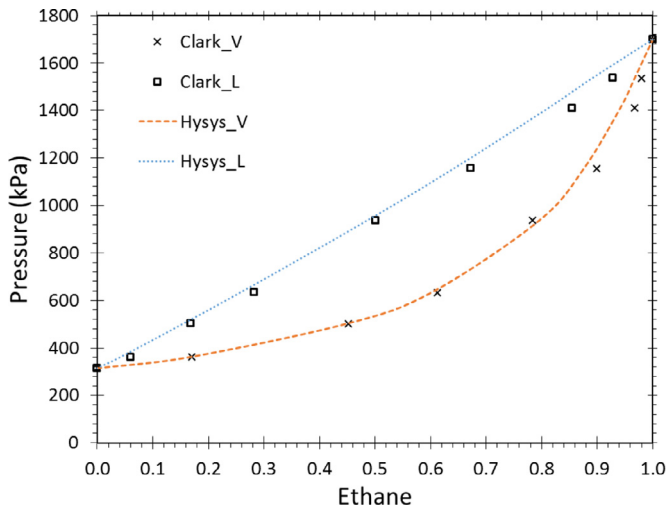


**Fig. 4.** Vapor–liquid equilibrium data for the system ethane/propane at  $T = 13.15$  °C obtained from Aspen Hysys® and from literature (Clark and Stead, 1988).

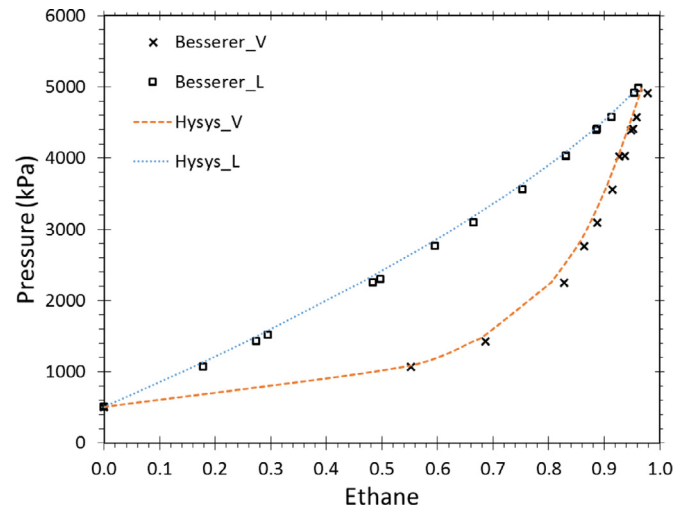


**Fig. 5.** Vapor–liquid equilibrium data for the system ethane/isobutane at  $T = 38.1$  °C obtained from Aspen Hysys® and from literature (Besserer and Robinson, 1973).

prediction is critical for the simulation of cycles operating with mixed refrigerants. To validate these data, bubble and dew points of the mixtures were calculated for the entire range of composition for pressures found in experimental works described in the literature: Clark and Stead (1988) for the systems ethane/propane, ethane/n-butane and propane/n-butane; Besserer and Robinson (1973) for the system ethane/isobutane; Hipkin (1966) for the system propane/isobutane. A comparison between simulated and experimental data was done and a good agreement was observed for all systems studied.

Figs. 4 and 5 present the results for the systems ethane/propane and ethane/isobutane, respectively. As can be seen, vapor–liquid equilibrium data of the studied binary mixtures were well modeled by the thermodynamic package of PR-EOS using Aspen HYSYS® since simulated and experimental data are very close to each other. Fig. 5 presents vapor–liquid equilibrium data for the system ethane/isobutane at 38.1 °C and since this temperature is above the critical temperature of pure ethane, it was not possible to obtain VLE points in the region close to pure ethane (as reported by Besserer and Robinson (1973)).

**Table 4**  
Input data and outputs of a FTVI operating with R290 from Redón et al. (2014) and this work.

Input Data	Output data			
		Redón et al. (2014)	This work	Deviation (%)
$T_{\text{cond}} (^{\circ}\text{C}) = 65$	$x_{\text{inj}}$	0.2844	0.2991	5.2
$T_{\text{evap}} (^{\circ}\text{C}) = -8$	$Sh_{\text{int}} (^{\circ}\text{C})$	6.8	6.12	10.0
$T_5 (^{\circ}\text{C}) = 60$	$T_{\text{discharge}} (^{\circ}\text{C})$	74.5	73.99	0.7
$T_1 (^{\circ}\text{C}) = -3$	COP (kW)	3.888	3.868	0.5
$P_3$ (kPa) = 1037				
$\eta_{\text{comp}}(\%) = 100$				
$Q_h$ (kW) = 15.98				

After validating thermodynamic data and properties for pure refrigerants and binary systems, the results of the simulated cycle itself were compared to the ones reported by Redón et al. (2014) that have presented results for ideal compressors and for real systems as well. For the validation of the simulation of the FTVI cycle, we have compared the results for the case of ideal compressors. Among several different scenarios, these authors modeled a FTVI heat pump operating with pure propane (R290) as refrigerant, in the conditions described on Table 4.

The evaluated results were COP, compressor discharge temperature ( $T_{\text{discharge}}$ ), intermediate superheating – which is the difference between the temperature in stream #3 and the saturation temperature at the same pressure ( $Sh_{\text{int}}$ ), injection ratio – which is the ratio between molar flows of streams #8 and #5 ( $x_{\text{inj}}$ ). Results for the COP and  $T_{\text{discharge}}$  obtained from Aspen Hysys<sup>®</sup> presented a deviation less than 1% from the ones presented by Redón et al. (2014). Deviations of the  $x_{\text{inj}}$  and  $Sh_{\text{int}}$  were, respectively, 5.2% and 10%. Even with slightly higher deviations for the last two properties, the results obtained with the simulation in Aspen Hysys<sup>®</sup> were considered in good agreement with the ones from the literature. Divergences could be due to the thermodynamic model used by Redón et al. (2014) or other modeling considerations not specified in their paper.

Considering all the results obtained from the model validation process, the simulator and the thermodynamic package chosen to simulate both VCC and FTVI cycles operating with hydrocarbons were considered reliable for the purpose of this work. Therefore, simulations and optimization of several operating scenarios were performed and the results are presented as follow.

### 3. Optimization

In order to find the most efficient operating configuration for the FTVI, an optimization algorithm was followed for each evaluated composition. The methodology used in the optimization procedure consisted of the following stages: 1 – a fixed cooling rate was determined for the application studied; 2 – a heat exchange fluid was chosen (water/ethanol solution) and its temperatures in the evaporator were also fixed (inlet temperature was 8.4 °C and outlet temperature was -4.0 °C); 3 – a specific composition for the mixed refrigerant was chosen and finally, 4 – an optimization procedure seeking a maximum COP was performed, considering these initial conditions. In this optimization procedure, manipulated variables were: mixed refrigerant temperature at stream #8 ( $T_8$ ), saturated vapor temperature in the condenser ( $T_{4,\text{vsat}}$ ) and expansion ratio in the first valve.

The closer the condenser temperature is from the one in the evaporator, the highest the cycle efficiency. However, due to the defined constraint of minimum temperature approach in both heat exchangers (5 °C) and the specific temperature glide of each refrigerant composition, the feasible closest temperatures varied from one scenario to another.

The objective function was defined as the maximization of the coefficient of performance (COP), calculated by Eq. (2) for the VCC and Eq. (3) for the FTVI.  $\dot{Q}_{\text{evaporator}}$  is the cooling capacity of the system;  $\dot{W}_{\text{compressor}}$  is the compressor power, which in the case of the FTVI is divided in two compression stages ( $\dot{W}_{\text{compressor}} = \dot{W}_{\text{comp1}} + \dot{W}_{\text{comp2}}$ ).

Optimization was carried out using Matlab<sup>®</sup> version R2013a, which allows online communication with the simulation built in Aspen Hysys<sup>®</sup>. *fmincon* (constrained nonlinear minimization) was selected as the most suitable among the available optimization functions in Matlab<sup>®</sup> because it allows objective function minimization and constraint addition. As there is no correspondent maximization function, COP with a negative sign was minimized to find the maximum cycle performance. The only constraints were minimum temperature approach of 5.0 °C in both heat exchangers.

The *Interior Point* algorithm was selected since it presented a better convergence for a wider boundary range when compared to the *SQP* algorithm. The input parameters for the optimization set up were: maximum iterations (400), maximum function evaluation ( $10^6$ ), function tolerance, step tolerance ( $X$ ) and constraint tolerance ( $10^{-6}$ ), finite differences perturbation between ( $10^{-2}$  and 10). For the other parameters, default values were used.

All the results presented in the next item of this work are for the optimized operating configuration of the FTVI. For comparison, VCC was evaluated at the same conditions of the optimized FTVI for each refrigerant composition.

Besides COP results, refrigerant glide temperature in evaporator was analyzed as well, aiming to evaluate the adequacy of the refrigerant to the industrial application chosen. The more the temperature profiles of fluids exchanging heat are similar, the smaller the mean temperature difference, leading to a reduction in irreversibility related to heat transfer (Mulroy et al., 1994; Radermacher and Hwang, 2005; Heberle et al., 2012). In this work, temperature glide matching was evaluated by comparing the refrigerant temperature glide with the Heat Exchange Fluid (HXF) temperature difference along the evaporator. HXF inlet and outlet temperatures are defined as a function of the application and in this work they are 8.4 °C and -4 °C ( $\Delta T_{\text{HXF}} = 12.4$  °C).

The third parameter evaluated is the refrigerant mass flow rate. The smaller it is, less refrigerant will be charged in the system and circulate in it, reducing the effects of explosions or fire due to its flammable nature and the necessity of higher compressor power and greater heat exchangers' areas. Pressure drop in pipes and heat exchangers will also be decreased if refrigerant mass flow rate is reduced (Corberán et al., 2008).

### 4. Results and discussion

For all results presented in this section, *composition* refers to the mass fraction of the lightest (more volatile) component in mixed refrigerant in stream #5, defined as the basis of calculation. Results for COP, temperature glide in evaporator and mass flow rate are presented and analyzed as a function of this com-

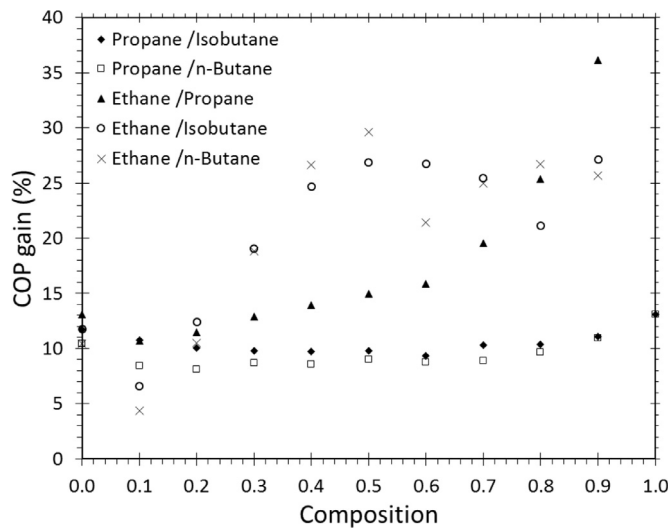


Fig. 6.  $COP_{gain}$  of FTVI related to VCC for each HC pair and composition.

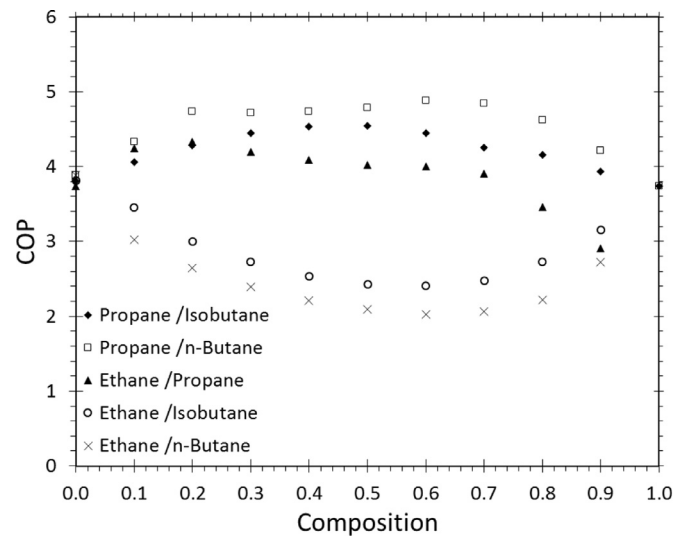


Fig. 7. Maximum COP for each refrigerant composition in FTVI.

position. For the systems involving ethane, missing points corresponding to pure ethane are due the fact that it is not feasible to use it as a refrigerant because its critical temperature is below the output temperature of the cooling water in the condenser.

#### 4.1. Comparison FTVI versus VCC

Cycle performance between FTVI and VCC was compared for each composition studied, taken at their optimum temperatures and ER (when applicable).  $COP_{gain}$  is given by Eq. (7) and the results are shown in Fig. 6.

$$COP_{gain}(\%) = \left( \frac{COP_{FTVI} - COP_{VCC}}{COP_{VCC}} \right) \times 100 \quad (7)$$

For all scenarios evaluated, FTVI always presents a better COP when compared with the VCC at the same fixed operating conditions, but no correlations of the results obtained could be detected for the systems studied. For the composition range studied, the great majority of the results for  $COP_{gain}$  are between 5% and 15%. These values are below the ones reported by d' Angelo et al. (2016) and indicate that a more detailed evaluation is required in order to determinate if the FTVI refrigeration system would be also economically viable, since it presents higher equipment cost and more complex operation control.

The improvement observed with the use of the FTVI cycle is due to the expansion in the upper stage valve, followed by the flash tank, which allows a fraction of the total refrigerant flow to skip the first compression stage, leading to a reduction of the total required work. The relative improvement reached with FTVI, though, varied from one composition to another. The greatest difference observed was 36% for the mixture ethane/propane 90/10 wt%.

#### 4.2. Comparison between refrigerant pairs

##### 4.2.1. Coefficient of performance

Results for the COP as a function of mixed refrigerant mass composition for the five studied pairs of refrigerants are presented at Fig. 7, only for FTVI. Missing points correspond to pure ethane, which is not feasible as a refrigerant in the proposed scenario because its critical temperature is below the output temperature of cooling water in the condenser. The system with the highest COP is R290/R600 60/40 wt% presenting a COP of 4.88. When this system was used in a VCC, COP was 4.49, representing a  $COP_{gain}$  of 8.7% as calculated by Eq. 7 when a FTVI is used.

According to McLinden and Radermacher (1987), when temperatures of evaporator inlet and saturated vapor in the condenser are the ones fixed and chosen as reference, the curve of COP as a function of mixed refrigerant composition should present a maximum behavior for any system at a constant expansion ratio. However, in this work only the minimum temperature approach of 5 °C at the heat exchangers was fixed in the simulations, allowing temperature variation at the points mentioned before and the expansion ratio as well. Therefore, the results do not exhibit the same trend because, depending on the combination of the variables, the behavior of COP may vary between the studied pairs. Refrigerants mixtures led to a better COP when comparing to their pure components for pairs formed by subsequent components of the homologous series: ethane/propane, propane/n-butane and propane/isobutane.

Heat source and sink temperatures are key-variables for the maximum efficiency of a thermodynamic cycle and different for each of the systems and compositions studied. This accounts for part of the COP relative deterioration, especially for n-butane/ethane and isobutane/ethane mixtures. Ethane vapor pressure is significantly higher than butane's, which leads to a wide temperature glide along the mixture evaporation.  $\Delta T_{refri} (T_1 - T_8)$  in evaporator was greater than 30 °C for some compositions (see Fig. 8), which makes the evaporator inlet temperature too low in order to not violate the constraint of  $\Delta T_{min} \geq 5$  °C. The same applies for the condenser, demanding high outlet temperatures at the second compression stage. For this reason, the minimum possible temperature difference between heat source and sink is much higher for the zeotropic mixture than for the pure refrigerant, leading to a significant decrease in COP.

The best COP (4.88) was observed for the mixed refrigerant propane/n-butane 60/40 wt%, with an expansion ratio of 37% in the upper stage valve. Values for temperature, pressure, enthalpy and other variables for each stream in this scenario are presented in Table 5. When compared to other mixtures, propane/n-butane has presented a higher efficiency along all the composition range. Optimal ER for this refrigerant pair are between 37% and 53%.

##### 4.2.2. Temperature glide

Temperature glide, that is the difference between refrigerant inlet and outlet temperatures in evaporator ( $\Delta T_{evaporator} = T_1 - T_8$ ) is compared to that of the heat exchange fluid ( $\Delta T_{HXF} = 12.4$  °C) in Fig. 8. Ethane/propane and propane/n-butane mixtures, both with 30 to 70 wt% of propane, presented a temperature glide in the

**Table 5**  
Results for FTVI cycle process streams with mixed refrigerant 60/40 wt% propane/n-butane at optimal operating conditions, with ER = 37%.

Evaporator Condenser	Heat load (kJ h <sup>-1</sup> )				Power (kJ h <sup>-1</sup> )					
	3600 4337				Compressor 1		Compressor 2			
Process stream	1	2	3	4	4 <sub>vsat</sub>	5	6	7	8	9
Temperature (°C)	3.38	33.16	30.97	50.10	42.11	30.05	13.89	13.89	-9.40	13.89
Pressure (kPa)	234	501	501	791	791	791	501	501	234	501
Flow rate (kg h <sup>-1</sup> )	10.13	10.13	11.45	11.45	11.45	11.45	11.45	10.13	10.13	1.32
Composition (wt%)	57	57	60	60	60	60	60	57	57	83
Vapor fraction	1.00	1.00	1.00	1.00	1.00	0.00	0.12	0.00	0.15	1.00
Specific enthalpy (kJ kg <sup>-1</sup> )	-2320	-2277	-2286	-2259	-2275	-2638	-2638	-2675	-2675	-2357
Specific entropy (kJ kg <sup>-1</sup> °C <sup>-1</sup> )	2.87	2.90	2.92	2.94	2.89	1.71	1.72	1.54	1.55	3.10

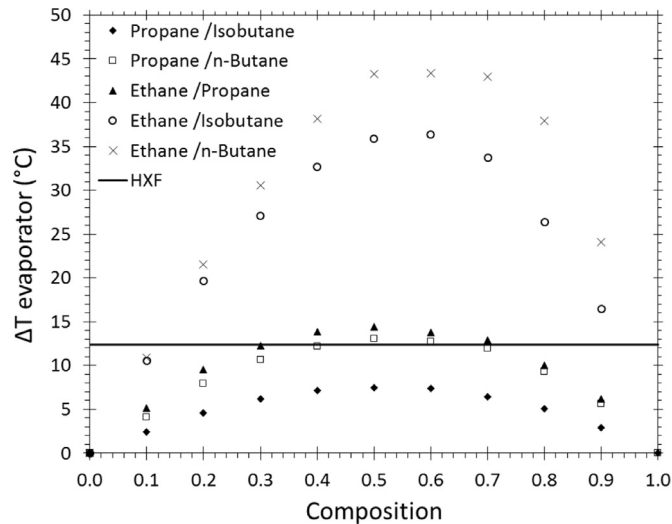


**Fig. 8.** Temperature glide in evaporator for each system and for the HXF.

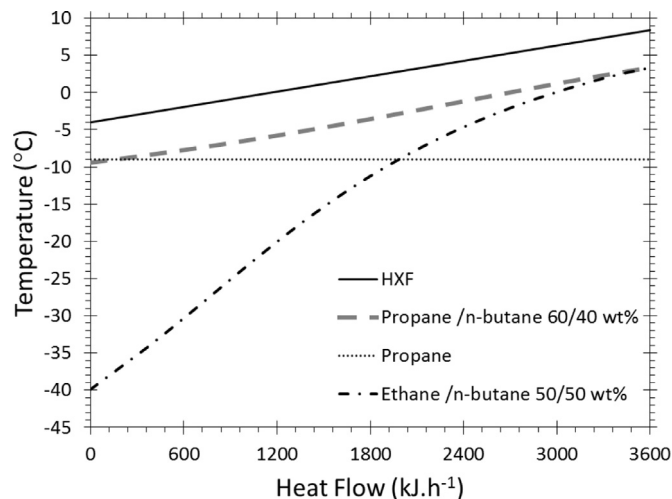


**Fig. 9.** Comparison between temperature profiles in the evaporator of FTVI cycle.

evaporator which is the closest to  $\Delta T_{HXF}$ . In order to better illustrate how temperature profiles in the evaporator are affected, three of them were plotted in Fig. 9 and compared with the HXF's.

Mulroy et al. (1994) have shown that an improvement of the COP of the refrigeration cycle can be achieved when temperature profiles of the refrigerant mixture and the heat transfer fluid are matched. Indeed this can be seen in Fig. 9 that shows a better temperature glide match for the system propane/n-butane 60/40 wt% which was the one with the greatest COP. This is also

**Table 6**  
Specific evaporation enthalpy of pure component at -10 °C and 0 °C (REFPROP®).

$\Delta h_{vap}$ (kJ kg <sup>-1</sup> )	-10 °C	0 °C
Ethane	336.0	302.6
Propane	388.3	374.9
n-Butane	394.0	385.3
Isobutane	363.5	354.3

related to the reduction of the irreversibilities due to smaller temperature differences between the working fluid and the heat exchange fluid during the heat exchange process (Heberle et al. 2012, Deethayat et al., 2015) which may be obtained with the use of a zeotropic mixed refrigerant.

Pure propane evaporates at constant temperature, so temperature difference between the fluids is equal to  $\Delta T_{min} = 5$  °C at one side of the heat exchanger and increases until  $(\Delta T_{min} + \Delta T_{HXF})$  at the other side, considering a counter-current flow. Ethane/n-butane 50/50 wt% presented the widest temperature glide in evaporator and a nonlinear profile, as shown in Fig. 9. Both behaviors increase irreversibility associated to heat exchange process, representing a negative contribution to the cycle's performance. According to Domanski et al. (1993), temperature profiles should be as parallel as possible, allowing the temperature difference between fluids to be constant - as was observed for the mixture propane/n-butane 60/40 wt%. For the same logarithmic mean temperature difference, parallel profiles correspond to the lowest entropy generation (Radermacher and Hwang, 2005). This example shows why the use of non-azeotropic mixtures is positive when the application requires sensible heat removal. Ideal temperature glide in evaporator depends on the application. In refrigeration systems designed to keep constant temperature, the use of pure refrigerants is better; for processes in which a temperature stream must be significantly reduced, mixtures with wider evaporation glide might be more interesting.

#### 4.2.3. Refrigerant mass flow rate

The third analyzed parameter was the total refrigerant mass flow rate of the system and stream #5 was chosen once again as the reference. As a 1 kW refrigeration load was fixed, refrigerant mass flow rate will depend on the specific evaporation enthalpy of refrigerants. Table 6 presents the values of these specific evaporation enthalpy for pure refrigerants at two different temperatures. Fig. 10 presents the mass flow rate in stream #5 as a function of mixed refrigerant composition in the FTVI cycle.

The specific evaporation enthalpy ( $\Delta h_{vap}$ ) of ethane is lower than the one of the other hydrocarbons, demanding higher refrigerant mass flow rate of mixtures that involve this component. However, from 30 to 90 wt% of ethane, ethane/isobutane mixture is not the one with greatest values for this variable, even though these are the components with lower  $\Delta h_{vap}$  of all. To understand

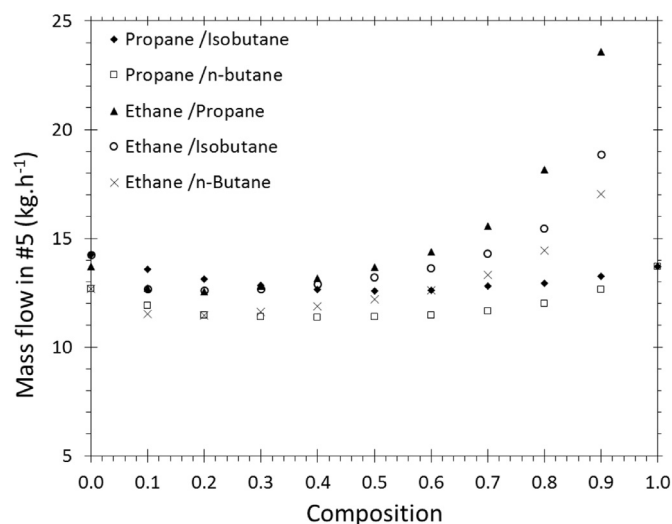


Fig. 10. Mass flow rate in stream #5 as a function of mixed refrigerant composition in FTVI cycle.

this result, the temperature glide in evaporator must be included in the analysis. When the glide exists, the vapor fraction entering the evaporator and vapor formed along it is heated to a higher outlet temperature. As the temperature changes, heat is also absorbed by the refrigerant vapor, contributing to the refrigeration capacity of the cycle. Both factors combined – specific evaporation enthalpy and temperature glide – makes ethane/propane the refrigerant pair with higher mass flow rates for systems containing more than 30 wt% of ethane.

As shown in Fig. 10, the refrigerant pair with the best results for mass flow rate was propane/n-butane – the same with the best COP. Total mass flow rate has shown a small variation as a function of the composition for this pair. In addition, a minimum point behavior was observed for all refrigerant pair (blends require lower mass flow rate than pure refrigerants), which is due to the non azeotropic mixture temperature glide, as explained.

## 5. Conclusions

In this paper, a study of a FTVI refrigeration cycle operating with a zeotropic mixture of natural refrigerants is presented trying to determine the best mixed refrigerant composition and operating conditions that lead to the maximum COP, through an optimization procedure. The performance of a traditional VCC was compared to the one of the FTVI at the same conditions.

Mixed refrigerants studied were binary mixtures involving four different hydrocarbons: ethane, propane, n-butane and isobutane. These systems were simulated and validated, concluding that the simulator was suitable to evaluate the behavior of the cycles, allowing finding the best operating condition after the optimization procedure.

The following conclusions can be drawn from this study:

- Comparison between the coefficients of performance of both cycles confirmed that the FTVI cycle always presents a COP higher than the one of a VCC, at the same operating conditions for a fixed cooling capacity.
- FTVI however shows some smaller disadvantages when compared to the VCC, considering its greater complexity and equipment required. A detailed economic analysis should be done in order to define whether an FTVI system is economically viable. This feasibility depends not only on the refrigerant used, but also on the application considered.

- Among mixed refrigerants studied the pair propane/n-butane 60/40 wt% presented the greatest COP for both VCC and FTVI cycles, respectively, 4.49 and 4.88. This refrigerant pair was also the one that presented the lowest mass flow rate and it was considered the most suitable for the application proposed in this study.
- Ethane/propane and propane/n-butane mixtures presented the best temperature glide matching in the evaporator. It was observed that when the temperatures of the secondary fluid in the heat exchanger are fixed, refrigerant temperature glide becomes an important evaluation parameter for the cycle, influencing the COP and the total mass flow rate required.
- The use of zeotropic mixed refrigerants allows a better temperature glide match with the heat exchange fluid, as a function of refrigerant composition, reducing irreversibilities during the heat exchange process, increasing the thermodynamic performance of the cycle.
- Considering the fact that natural refrigerants present low environmental impact, together with their availability and low cost, zeotropic mixtures of natural refrigerants present a great potential to be used in refrigeration systems.
- This study brings contributions towards understanding the advantages of using zeotropic mixtures of natural refrigerants (hydrocarbons) in both conventional VCC and alternative FTVI refrigeration cycle.

## Acknowledgments

The authors acknowledge the financial support from the National Council for Scientific and Technological Development (Conselho Nacional de Desenvolvimento Científico e Tecnológico – CNPq) through the research scholarship granted (Process 152390/2015-4).

## References

- Araújo, H.V., Carvalho, S.M.R., D'Angelo, J.V.H., 2016. Exergy analysis of a vapor injection refrigeration system with flash tank using refrigerant mixture R290 / R600a. In: Proceedings of Modelling, Simulation and Identification/841: Intelligent Systems and Control – MSI2016 doi:10.2316/P.2016.840-050.
- AspenTech, 2018. Aspen HYSYS Help Section. Aspen Technology, Inc., Burlington, MA, USA <https://www.aspentech.com/>.
- Besserer, G.J., Robinson, D.B., 1973. Equilibrium-phase properties of isobutane-ethane system. J. Chem. Eng. Data 18, 301–304. doi:10.1021/je60058a003.
- Calm, J.M., 2008. The next generation of refrigerants – Historical review, considerations, and outlook. Int. J. Refrig. 31, 1123–1133. doi:10.1016/j.ijrefrig.2008.01.013.
- Campbell, J.M., 1992. Gas Conditioning and Processing – Volume 2: The Equipment Modules, Seventh ed. Campbell Petroleum Series, Bound, pp. 978–9992925805 ISBN-13.
- Clark, A.Q., Stead, K., 1988. (Vapour + liquid) phase equilibria of binary, ternary, and quaternary mixtures of CH<sub>4</sub>, C<sub>2</sub>H<sub>6</sub>, C<sub>3</sub>H<sub>8</sub>, C<sub>4</sub>H<sub>10</sub>, and CO<sub>2</sub>. J. Chem. Thermodyn. 20, 413–427. doi:10.1016/0021-9614(88)90178-4.
- Corberán, J.M., Segurado, J., Colbourne, D., González, J., 2008. Review of standards for the use of hydrocarbon refrigerants in A/C, heat pump and refrigeration equipment". Int. J. Refrig. 31, 748–756. doi:10.1016/j.ijrefrig.2007.12.007.
- D'Angelo, J.V.H., Aute, V., Radermacher, R., 2016. Performance evaluation of a vapor injection refrigeration system using mixture refrigerant R290/R600a. Int. J. Refrig. 65, 194–208. doi:10.1016/j.ijrefrig.2016.01.019.
- Deethayat, T., Kiatsiriroat, T., Thawonngamyingsakul, C., 2015. Performance analysis of an organic Rankine cycle with internal heat exchanger having zeotropic working fluid. Case Stud. Therm. Eng. 6, 155–161. doi:10.1016/j.csite.2015.09.003.
- Didion, D.A., Bivens, D.B., 1990. Role of refrigerant mixtures as alternatives to CFCs. Int. J. Refrig. 13, 163–175. doi:10.1016/0140-7007(90)90071-4.
- Domanski, P.A., Mulroy, W.J., Didion, D.A., De, C., 1993. Glide matching with binary and ternary zeotropic refrigerant mixtures Part 2. A computer simulation. Int. J. Refrigeration. 17, 226–230. doi:10.1016/0140-7007(94)90038-8.
- Heberle, F., Preißinger, M., Brüggemann, D., 2012. Zeotropic mixtures as working fluids in organic Rankine cycles for low-enthalpy geothermal resources. Renew. Energy 37, 364–370. doi:10.1016/j.renene.2011.06.044.
- Heggs, P.J., 1989. Minimum temperature difference approach concept in heat exchangers network. Heat Recover. Syst. CHP 9, 367–375. doi:10.1016/0890-4332(89)90089-6.
- Heo, J., Jeong, M.W., Kim, Y., 2010. Effects of flash tank vapor injection on the heating performance of an inverter-driven heat pump for cold regions. Int. J. Refrig. 33, 848–855. doi:10.1016/j.ijrefrig.2009.12.021.

- Hipkin, H., 1966. Experimental vapor–liquid equilibrium data for propane–isobutane. *AIChE J.* 117, 1964–1967. doi:10.1002/aic.690120317.
- IIR - International Institute of Refrigeration, 2015. Twenty-ninth Informatory Note on Refrigerating Technologies/November 2015 – the role of Refrigeration in the Global Economy. [http://www.iifir.org/userfiles/file/publications/notes/NoteTech\\_29\\_EN.pdf](http://www.iifir.org/userfiles/file/publications/notes/NoteTech_29_EN.pdf)
- McLinden, M.O., Radermacher, R., 1987. Methods for comparing the performance of pure and mixed refrigerants in the vapour compression cycle. *Int. J. Refrig.* 10, 318–325. doi:10.1016/0140-7007(87)90117-4.
- Mohanraj, M., Jayaraj, S., Muraleedharan, C., Chandrasekar, P., 2009. Experimental investigation of R290/R600a mixture as an alternative to R134a in a domestic refrigerator. *Int. J. Therm. Sci.* 48, 1036–1042. doi:10.1016/j.ijthermalsci.2008.08.001.
- Mulroy, W.J., Domanski, P.A., Didion, D.A., 1994. Glide matching with binary and ternary zeotropic refrigerant mixtures – part I. An experimental study. *Int. J. Refrig.* 17, 220–225. doi:10.1016/0140-7007(94)90037-X.
- Oh, J.-S., Binns, M., Park, S., Kim, J.-K., 2016. Improving the energy efficiency of industrial refrigeration systems. *Energy* 112, 826–835. doi:10.1016/j.energy.2016.06.119.
- Palm, B., 2008. Hydrocarbons as refrigerants in small heat pump and refrigeration systems – a review. *Int. J. Refrig.* 31, 552–563. doi:10.1016/j.ijrefrig.2007.11.016.
- Park, K.-J., Jung, D., 2007. Thermodynamic performance of HCFC22 alternative refrigerants for residential air-conditioning applications. *Energy Build.* 39, 675–680. doi:10.1016/j.enbuild.2006.10.003.
- Park, C., Lee, H., Hwang, Y., Radermacher, R., 2015. Recent advances in vapor compression cycle technologies. *Int. J. Refrig.* 60, 118–134. doi:10.1016/j.ijrefrig.2015.08.005.
- Peng, D.Y., Robinson, D.B., 1976. A new two-constant equation of state. *Ind. Eng. Chem. Fundam.* 15, 59–64. doi:10.1021/i160057a011.
- Qi, H., Liu, F., Yu, J., 2017. Performance analysis of a novel hybrid vapor injection cycle with subcooler and flash tank for air-source heat pumps. *Int. J. Refrig.* 74, 540–549. doi:10.1016/j.ijrefrig.2016.11.024.
- Radermacher, R., Hwang, Y., 2005. *Vapor Compression Heat Pumps with Refrigerant Mixtures*, First ed CRC Press, Boca Raton ISBN-13: 978-0-8493-3489-4.
- Redón, A., Navarro-Peris, E., Pitarch, M., González-Macia, J., Corberán, J.M., 2014. Analysis and optimization of subcritical two-stage vapor injection heat pump systems. *Appl. Energy* 124, 231–240. doi:10.1016/j.apenergy.2014.02.066.
- Tello-Oquendo, F.M., Navarro-Perris, E., González-Maciá, J., 2018. A comprehensive study of two-stage vapor compression cycles with vapor-injection for heating applications, taking into account heat sink of finite capacity. *Int. J. Refrig.* 93, 52–64. doi:10.1016/j.ijrefrig.2018.05.039.
- Xu, X., Hwang, Y., Radermacher, R., 2011. Refrigerant injection for heat pumping/air conditioning systems: literature review and challenges discussions. *Int. J. Refrig.* 34, 402–415. doi:10.1016/j.ijrefrig.2010.09.015.
- Xu, S., Fan, X., Ma, G., 2017. Experimental investigation on heating performance of gas-injected scroll compressor using R32, R1234yf and their 20wt%/80wt% mixture under low ambient temperature. *Int. J. Refrig.* 75, 286–292. doi:10.1016/j.ijrefrig.2017.01.010.
- Xu, S., Niu, J., Cui, Z., Ma, G., 2018. Experimental research on vapor-injected heat pump using injection subcooling. *Appl. Therm. Eng.* 136, 674–681. doi:10.1016/j.applthermaleng.2018.03.028.
- Zheng, N., Wei, J., 2018. Performance analysis of a novel vapor injection cycle enhanced by cascade condenser for zeotropic mixtures. *Appl. Therm. Eng.* 139, 166–176. doi:10.1016/j.applthermaleng.2018.04.135.